of a coordination number of 6 for the mononuclear complexes in solution, one should certainly see a dramatic increase in the difference between the successive binding constants of M(II) to H_2L and HL and M(II) to L. Nitrogen coordination higher than 3 is unlikely in MH_2L or MHL, where M(II) is expected to bind to one BAMP unit while the proton(s) is (are) located on the opposite binding moiety. For the macrocycle O2-BISBAMP, it is seen that the binding constants of M(II) to H_iL increase steadily by an average value of 1.8 log units as i decreases. For O-BISBAMP, there is also an increase, which is larger for the first step (MH_2L–MHL) than the second. For a change in coordination from one to two BAMP units, a much larger increase should be expected in going from MH_iL to ML. Therefore, there is strong evidence from solution studies that the structure of the mononuclear complex is solution can be represented by the metal ion bound to one and only one terdentate BAMP unit. Solvation of the ether oxygens by water molecules might prevent the two BAMP moieties from binding to the same metal, a process that would require at least partial desolvation of the ether oxygens.

Acknowledgment. R.M. acknowledges a Convention Ciffre Scholarship from the French Ministry of Research and Technology. Appreciation is expressed for financial support from the Office of Naval Research, under Grant No. N00014-88K-0451.

Registry No. **4**, 75620-07-4; **4**·4HCl, 123726-19-2; **6**, 75620-06-3; Co, 7440-48-4; Cu, 7440-50-8; Zn, 7440-66-6; Ni, 7440-02-0; Pb, 7439-92-1; 2,6-pyridinedicarboxaldehyde, 5431-44-7; 1,8-diamino-3,6-dioxaoctane, 929-59-9.

Contribution from the Laboratoire de Cristallochimie et de Chimie Structurale, UA (CNRS) 424, Institut le Bel, Université Louis Pasteur, 4, rue B. Pascal, F-67070 Strasbourg, France, and Institut für Physik, Medizinische Universität, Ratzeburger Allee 160, D-2400 Lübeck 1, FRG

Synthesis, Structure, and Spectroscopic Properties of Five-Coordinate Mercaptoiron(II) Porphyrins. Models for the Reduced State of Cytochrome P450

M. Schappacher,[1] L. Ricard,[1] J. Fischer,[1] R. Weiss,*[,1] R. Montiel-Montoya,[2] E. Bill,[2] and A. X. Trautwein*[,2]

Received November 29, 1988

The five-coordinate, high-spin (S = 2) (ethanethiolato)- and (tetrafluorobenzenethiolato)iron(II) "picket-fence" porphyrin derivatives [Fe($TP_{piv}P$)(SC_2H_5)][Na(C222)] (**1**), [Fe($TP_{piv}P$)(SC_6HF_4)][Na(C222)] (**2**), and [Fe($TP_{piv}P$)(SC_6HF_4)][Na(C18c6)] (**3**) have been synthesized and characterized. The X-ray structure of the chlorobenzene solvate of **1** has been determined. [Fe($TP_{piv}P$)(SC_2H_5)][Na(C222)]·C_6H_5Cl ($C_{90}H_{110}N_{10}O_{10}$ NaSClFe) crystallizes in the monoclinic system with a = 23.394 (7) Å, b = 21.762 (7) Å, c = 17.890 (6) Å, β = 103.62 (2)°, Z = 4, and space group $P2_1/n$ (Cu Kα radiation). The average Fe–N_p bond distance is 2.074 (10) Å. The displacement of iron out of the 4 Np mean plane is 0.44 Å. The ethanethiolato axial ligand of iron lies in the molecular cavity formed by the four pivalamido groups of the picket-fence porphyrin. The Fe–S bond distance of 2.324 (2) Å is in complete agreement with the Fe–S bond length found in the reduced ferrous state of cytochrome P450 by EXAFS spectroscopy. Experimental Mössbauer spectra of **1**–**3** exhibit isomer shifts that are typical for five-coordinate ferrous high-spin porphyrins and that are practically identical with that reported for reduced P450. Additionally the observed quadrupole splitting (ΔE_Q) of **1**–**3** is comparable to that of reduced P450, and especially the temperature dependence of ΔE_Q from **3** between 4.2 and 200 K is very similar to that of the reduced enzyme. The Mössbauer spectra measured under an applied field (6.4 T $\perp$ γ) in the temperature range 1.8–200 K were analyzed by the usual spin Hamiltonian formalism. The resulting zero-field splitting and hyperfine structure derived for **1** and **3**, respectively, are very close to what was found for reduced P450. Comparing the spectroscopic properties of five-coordinate mercaptoiron(II) porphyrins with those reported for the reduced state of cytochrome P450, we conclude that the cysteinate ligand remains bonded to iron in the ferrous state and is not protonated when reduction of the ferric to the ferrous state of P450 takes place.

Introduction

Both mammalian and bacterial cytochromes P450 show a common reaction cycle with four well-characterized isolable states.[3] The low-spin six-coordinate ferric resting state is converted to a high-spin five-coordinate state upon substrate binding. Reduction leads to the reduced ferrous state, in which iron is also five-coordinate. This form is converted to the oxy state by O_2 uptake. High-spin ferrous P450 is thus formed by electron transfer to the high-spin ferric enzyme substrate complex state.

Although the normal reaction cycle of chloroperoxidase (CPO) dose not involve the intermediacy of a ferrous derivative, such a state can be produced by anaerobic reduction of the high-spin ferric state of this enzyme.[3]

The spectroscopic properties of the reduced ferrous state of P450 and the reduced ferrous form of CPO have been extensively explored and have consistently been found to be quite similar to each other as well as to the properties of five-coordinate high-spin ferrous porphyrin thiolate model complexes.[4-15] The recent publications of the crystal structures of high-spin ferric $P450_{CAM}$[16] and that of the resting state of $P450_{CAM}$[17] have confirmed directly that a cysteinate ligand is bonded to iron in these two states of $P450_{CAM}$. EXAFS spectroscopy has been used to examine ferrous $P450_{CAM}$.[15] The EXAFS data together with the crystallographic results,[8] which we published several years ago for the thiolate model complex [Fe(TPP)(SEt)]$^-$, strongly suggested that the

(1) Université Louis Pasteur.
(2) Medizinische Universität.
(3) Dawson, J. H.; Sono, M. *Chem. Rev.* **1987**, *87*, 1255 and references therein.
(4) Keller, R. M.; Wüthrich, K.; Debrunner, P. G. *Proc. Natl. Acad. Sci. U.S.A.* **1972**, *69*, 2073.
(5) Champion, P. M.; Münck, E.; Debrunner, P. G.; Moss, T. H.; Lipscomb, J. D.; Gunsalus, I. C. *Biochim. Biophys. Acta* **1975**, *376*, 579.
(6) Chang, C. K.; Dolphin, D. *J. Am. Chem. Soc.* **1975**, *97*, 5948.
(7) Chang, C. K.; Dolphin, D. *Proc. Natl. Acad. Sci. U.S.A.* **1976**, *73*, 3338.
(8) Caron, C.; Mitschler, A.; Rivière, G.; Ricard, L.; Schappacher, M.; Weiss, R. *J. Am. Chem. Soc.* **1979**, *101*, 7401.
(9) Parmely, R. C.; Goff, H. M. *J. Inorg. Biochem.* **1980**, *12*, 269.
(10) Budyka, M. F.; Khenkin, A. M.; Shteinman, A. A. *Biochem. Biophys. Res. Commun.* **1981**, *101*, 615.
(11) Okubo, S.; Nozawa, T.; Hatano, M. *Chem. Lett.* **1981**, 1625.
(12) Battersby, A. R.; Howson, W.; Hamilton, A. D. *J. Chem. Soc., Chem. Commun.* **1982**, 1266.
(13) Schappacher, M.; Ricard, L.; Weiss, R.; Montiel-Montoya, R.; Gonser, U.; Bill, E.; Trautwein, A. X. *Inorg. Chim. Acta* **1983**, *78*, L9.
(14) Cramer, S. P.; Dawson, J. H.; Hodgson, K. O.; Hager, L. P. *J. Am. Chem. Soc.* **1978**, *100*, 7282.
(15) Hahn, J. E.; Hodgson, K. O.; Anderson, L. A.; Dawson, J. H. *J. Biol. Chem.* **1982**, *257*, 10934.
(16) Poulos, T. M.; Finzel, B. C.; Gunsalus, I. C.; Wagner, G. C.; Kraut, J. *J. Biol. Chem.* **1985**, *260*, 16122.
(17) Poulos, T. L.; Finzel, B. C.; Howard, A. J. *Biochemistry* **1986**, *25*, 5314.

0020-1669/89/1328-4639$01.50/0

cysteinate ligand in the enzyme substrate complex state of P450 is not protonated when the reduction of the ferric to the ferrous enzyme takes place.

In this paper, we report the synthesis and Mössbauer properties of several five-coordinate high-spin (thiolato)iron(II) porphyrins together with the X-ray structure of another five-coordinate (thiolato)iron(II) porphyrin species, [Fe($TP_{piv}P$)(SEt)]. The Fe–S bond distance of 2.324 (2) Å found in this complex is slightly shorter than that found[8] in $[Fe(TPP)(SEt)]^-$ and is in complete agreement with the distances found by EXAFS spectroscopy in the ferrous state of $P450_{CAM}$[15] and in the model compound $[Fe(OEP)SPr]^-$.[18]

Experimental Section

General Procedures. All experiments were done under an inert atmosphere either by Schlenk techniques or in a Vacuum Atmospheres drybox, unless otherwise stated. Solvent were rigorously purified and dried under argon. The free meso-$\alpha,\alpha,\alpha,\alpha$-tetrakis(*o*-pivalamidophenyl)porphyrin($TP_{piv}PH_2$) and the corresponding chloroiron(III) derivative were synthesized by literature methods.[19] Ethanethiol and 2,3,5,6-tetrafluorobenzenethiol were obtained from Aldrich. The sodium salt of ethanethiolate was prepared by the reaction of NaH (100 mg, 4.1 mmol) with a solution of C_2H_5SH (248 mg, 4 mmol) in benzene (20 mL). The mixture was stirred 24 h at ambient temperature. The white precipitate was filtered, washed with dry pentane, dried under vacuum, and stored in the drybox. The sodium salt of 2,3,5,6-tetrafluorobenzenethiol was prepared in dry THF. This solvent was first dried over sodium/benzophenone and distilled over $LiAlH_4$. NaH (480 mg, 20 mmol) was dissolved under argon in THF (50 mL). To this solution was added stepwise 2,3,5,6-tetrafluorobenzenethiol (5 g, 25 mmol). The mixture was stirred until no more hydrogen evolution was observed. The volume of the solution was then reduced by 50% by evaporation under vacuum. Dry pentane (50 mL) was then added. The resulting white precipitate was filtered, washed twice with pentane, dried for at least 3 h under vacuum, and stored in the drybox. The purity of the sodium thiolates was checked by IR spectroscopy.

Synthesis of [Fe($TP_{piv}P$)(SC_2H_5)][Na(C222)] (1). A solution of [Fe^{III}($TP_{piv}P$)Cl] (100 mg, 0.088 mmol) in freshly distilled and deaerated chlorobenzene (30 mL) was stirred for 1 h with zinc amalgam (1 mL) containing 5% zinc. After filtration a chlorobenzene solution (20 mL) of Kryptofix 222 (4,7,13,16,21,24-hexaoxa-1,10-diazabicyclo[8.8.8]hexacosane, Aldrich; 150 mg, 0.40 mmol) and sodium ethanethiolate (33 mg, 0.39 mmol) were added. The five-coordinate (thiolato)iron(II) porphyrin complex was precipitated by addition of dry pentane. Sodium ethanethiolate present in excess in the solution precipitated also under these conditions. Thus, the solid compounds obtained in this way always contained the mercaptoiron(II) porphyrin together with some 222-cryptated sodium thiolate. Single crystals containing a chlorobenzene molecule of solvation, suitable for X-ray studies, were obtained by slow diffusion of pentane into the chlorobenzene solutions that contained the iron porphyrin and 222-cryptated sodium ethanethiolate (vide infra). λ_{max} (C_6H_5Cl): 421, 533, 575, 625 nm.

Synthesis of [Fe($TP_{piv}P$)(SC_6HF_4)][Na(⊂222)] (2). This compound was obtained similarly from [Fe($TP_{piv}P$)Cl] (0.088 mmol), sodium tetrafluorobenzenethiolate, and 222 cryptand, however only as an oily precipitate. λ_{max}: 419, 530, 570, 605 nm.

Synthesis of [Fe($TP_{piv}P$)(SC_6HF_4)][Na(⊂18c6)] (3). [Fe^{III}($TP_{piv}P$)Cl] (100 mg, 0.088 mmol) dissolved in freshly distilled deaerated benzene (30 mL) was stirred for 1 h in the presence of zinc amalgam (1 mL) containing 5% zinc. After filtration, a benzene solution (20 mL) of sodium tetrafluorobenzenethiolate (86 mg, 0.39 mmol) containing the 18-crown-6 macrocyclic polyether (18c6; 105 mg, 0.40 mmol) was added. Slow evaporation under vacuum or diffusion of pentane yielded the crystalline five-coordinate [Fe($TP_{piv}P$)(SC_6HF_4)][Na(⊂18c6)] (3) complex. λ_{max} (C_6H_5Cl): 419, 530, 570, 605 nm.

X-ray Crystallography. Suitable dark-blue crystals of [Fe($TP_{piv}P$)(SC_2H_5)][Na(⊂222)]·C_6H_5Cl (1′) were obtained as described above for **1**. A systematic search in reciprocal space with a Philips PW1100/16 automatic diffractometer showed that crystals of 1′ belong to the monoclinic system. The unit-cell dimensions and their standard deviations were obtained and refined at room temperature with Cu Kα radiation (λ = 1.5405 Å) by using 25 carefully selected reflections and the standard Philips software. The corresponding results are given in Table I.

Table I. Crystallographic Data for [Fe($TP_{piv}P$)(SC_2H_5)][Na(⊂222)]·C_6H_5Cl (1′)

chem formula: $C_{90}H_{110}N_{10}O_{10}NaSClFe$	space group: $P2_1/n$ (No. 14)
fw: 1638.3	T = 22 °C
a = 23.394 (7) Å	λ = 1.5405 Å
b = 21.762 (7) Å	ρ_{calc} = 1.226 g cm^{-3}
c = 17.890 (6) Å	μ = 23.94 cm^{-1}
β = 103.62 (2)°	transmission coeff: 0.83–1.57
V = 8851.7 Å^3	$R(F_o)$ = 0.077
Z = 4	$R_w(F_o)$ = 0.103

A nearly parallelepipedic crystal of dimensions 0.35 × 0.44 × 0.45 mm^3 was cut out from a cluster of crystals, sealed in a Lindemann glass capillary, and mounted on a rotation-free goniometer head. All quantitative data were obtained from a Philips PW1100/16 four-circle automatic diffractometer controlled by a P852 computer, using graphite-monochromated radiation and standard software. The vertical and horizontal apertures in front of the scintillation counter were adjusted so as to minimize the background without loss of the net peak intensity at the 2σ level. Data were collected by using the $\theta/2\theta$ flying step-scan mode and were transferred to a PDP11/60 computer; for all subsequent computations the Enraf-Nonius SDP/PDP package[20] was used with the exception of a local data-reduction program. Three standard reflections measured every 1 h during the entire data-collection period showed no significant trend. The raw step-scan data were converted to intensities by using the Lehmann-Larsen[21] method and then corrected for Lorentz and polarization factors. Absorption corrections were applied by using the empirical method of Walker and Stuart.[22] The structure was solved by using Patterson and Fourier techniques. Oxygen atom O72, carbon atoms C74, C75, and C76, and the chlorine atom of the solvent are disordered over two positions. They were duplicated with occupancy factors of 0.5 based on relative peak heights. After refinement of the heavy atoms, difference-Fourier maps revealed maxima of residual electronic density close to the positions expected for hydrogen atoms; they were introduced in structure factor calculations by their computed coordinates (C—H=N—H = 0.95 Å) and isotropic temperature factors such that $B(H) = 1 + 1.3[B_{eqv}(C \text{ or } N)]$ Å^2 but not refined (C74′, C75′, C76′ hydrogens omitted). Full least squares minimizing $\sum w(|F_o| - |F_c|)^2$ converged to $R(F)$ = 0.077 and $R_w(F)$ = 0.103 ($\sigma^2(F^2) = \sigma^2(\text{counts}) + (pI)^2$). The unit-weight observation was 1.89 for p = 0.08. A final difference map revealed no significant maxima. The scattering factor coefficients and anomalous dispersion coefficients come from parts a and b of ref 23, respectively. Due to spurious failures of the low-temperature device, this structure was studied at room temperature. Consequently, the chemically equivalent bond lengths in the porphyrin and cryptate are spread over a somewhat larger range than in the porphyrin structures that we have studied at −100 °C. However, despite these larger ranges, all the chemically equivalent bond distances found are not significantly different at the 3σ level.

Mössbauer Spectroscopy. The Mössbauer spectrometer worked in the conventional constant-acceleration mode with a ^{57}Co/Rh source of ca. 1.8 GBq activity (Amersham Buchler). From calibration measurements we got a standard line width of 0.23 mm s^{-1}. Isomer shifts are given relative to metallic iron (α-Fe) at room temperature. The Mössbauer cryostats were a helium-bath cryostat (MD306, Oxford Instruments) and a superconducting magnet system with split coil geometry (Oxford Instruments). The γ beam could be transmitted parallel or perpendicular to the field. The sample temperature in the cryomagnet was regulated independent of the source temperature in a variable-temperature insert.

Results and Discussion

X-ray Structure. The asymmetric unit of the crystals of **1**·C_6H_5Cl (1′) contains one formula unit of [Fe($TP_{piv}P$)(SC_2H_5)][Na(⊂222)]·C_6H_5Cl. The molecular stereochemistry of the iron porphyrin anionic complex is displayed in Figure 1 together with the identifying labels used for all atoms. Figure 2 represents a projection of the porphyrin on the mean plane of

(18) Kau, L. S.; Svastits, E. W.; Dawson, J. H.; Hodgson, K. O. *Inorg. Chem.* **1986**, *25*, 4307.
(19) Collman, J. P.; Gagné, R. R.; Halbert, T. R.; Lang, G.; Robinson, W. T. *J. Am. Chem. Soc.* **1975**, *97*, 1427.
(20) Frenz, B. A. In *Computing in Crystallography*; Schenk, H., Olthof-Hazekamp, R., van Koningsveld, H., Bassi, C. G., Eds.; Delft University Press: Delft, The Netherlands, 1978; p 65.
(21) Lehmann, M. S.; Larsen, F. K. *Acta Crystallogr., Sect. A: Cryst. Phys., Diffr., Theor. Gen. Crystallogr.* **1974**, *A30*, 580.
(22) Walker, N.; Stuart, D. *Acta Crystallogr., Sect. A: Found. Crystallogr.* **1983**, *A39*, 158.
(23) (a) Cromer, D. T.; Waber, J. T. In *International Tables for X-Ray Crystallography*; Kynoch: Birmingham, England, 1974; Vol. IV, Table 2.2b. (b) *Ibid.* Table 2.3.1.

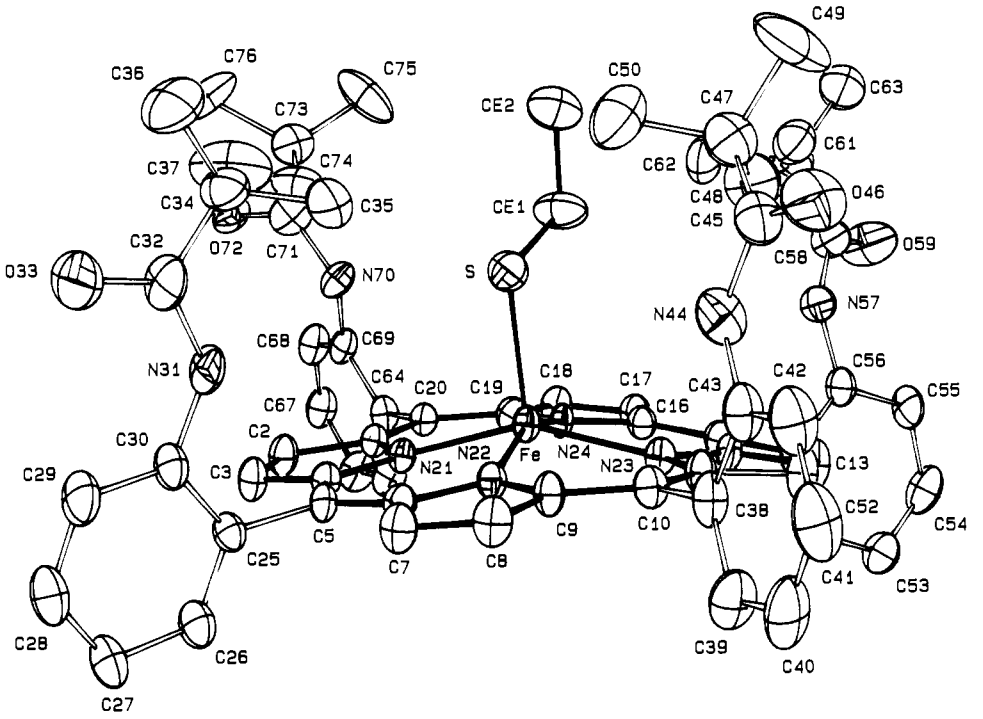

Figure 1. ORTEP plot and atom-numbering scheme for $[Fe(TP_{piv}P)(SC_2H_5)]^-$ in **1′**. Hydrogen atoms have been omitted for clarity. Thermal ellipsoids are at the 30% probability level.

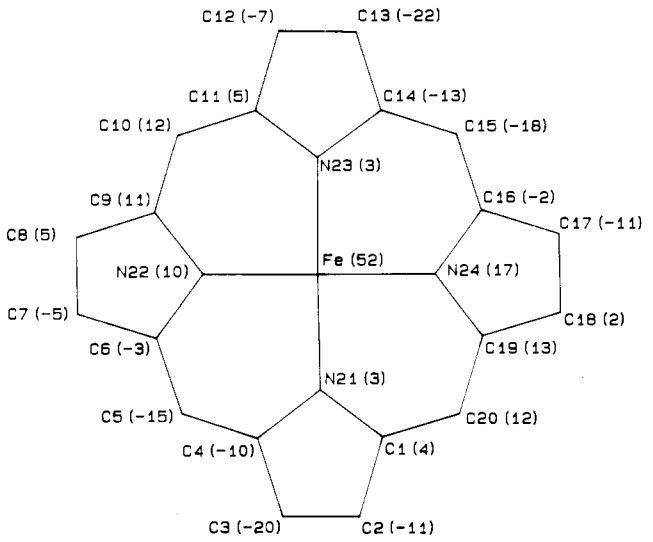

Figure 2. Formal diagram of the porphyrinato core. The numbers in parentheses indicate the perpendicular displacement for each atom in units of 0.01 Å from the mean plane of the 24-atom core.

this ring. The positional and thermal equivalent parameters are given in Table II. Selected bond distances and angles are given in Table III.

The iron atom is, as expected, five-coordinate, bonded to the four N_p nitrogens and a sulfur atom of the thiolate. The Fe–N_p distances range from 2.066 (4) to 2.088 (4) Å. The corresponding mean value is 2.074 (10) Å. The thiolate axial ligand is located inside the molecular cavity of the picket-fence porphyrin. This structure is very often found in five-coordinate picket-fence porphyrin complexes with anionic axial ligands.[24,25] The Fe–S bond length of 2.324 (2) Å is 0.046 (3) Å shorter than the Fe–S bond distance present in the five-coordinate 2,3,5,6-tetrafluorobenzenethiolate complex $[Fe(TP_{piv}P)(SC_6HF_4)][Na(\subset 18c6)]$ (**3**) (Fe–S = 2.370 (3) Å)[13] and identical with the iron(III)–sulfur bond length observed in $[Fe(PP(IX)DME)(SC_6H_4\text{-}p\text{-}NO_2)]$ (Fe–S = 2.324 (2) Å).[26] The shortening of the Fe–S bond length by 0.046 Å in **1**·C_6H_5Cl with respect to that in the 2,3,5,6-tetrafluorobenzenethiolate derivative **3** can be explained by the increased strength as axial ligand of alkanethiolates relative to that of aromatic thiolates. However, the Fe–S distance of 2.324 (2) Å present in $[Fe(TP_{piv}P)(SC_2H_5)]^-$ is also 0.036 Å shorter than the Fe–S bond length found in the very similar compound $[Fe(TPP)(SC_2H_5)][Na(\subset 222)]\cdot C_6H_5Cl$.[8] Presently, we have no plausible explanation to offer for this observation, except that in the $[Fe(TP_{piv}P)SC_2H_5)]^-$ ion the ethanethiolate lies in the molecular cavity formed by four pivalamido polarizing pickets. The displacement of the metal with respect to the mean plane of the porphyrinato nitrogens $\Delta(N_4)$ is also related to the strength of the axial ligand. Indeed, this displacement is larger in the ethanethiolate derivative ($\Delta(N_4)$ = 0.437 (1) Å) than in the tetrafluorobenzenethiolate derivative ($\Delta(N_4)$ = 0.42 Å). The corresponding displacement of 0.52 Å in $[Fe(TPP)(SC_2H_5)]^-$ again does not fit in this series.

The Fe–S bond length of 2.324 (2) Å observed in $[Fe(TP_{piv}P)(SC_2H_5)]^-$ compares well with the Fe–S bond distance found by EXAFS spectroscopy in the reduced ferrous state of $P450_{CAM}$ (Fe–S = 2.34 Å) and in the model complex $[Fe(OEP)SPr]^-$ (2.33 Å).[18] This Fe–S bond is in **1′** slightly tipped by 5.1 (3)° away from the normal to the 4 N_p porphyrin mean plane and by 6.1 (3)° with respect to the normal to the 24-atom-core mean plane. As is seen in Figure 2, the porphyrinato core has a domed conformation. This doming is also indicated by the separation of the 4 N_p mean plane and the 24-atom-core mean plane of 0.085 (1) Å. More doming is present in the ethanethiolate complex $[Fe(TPP)(SC_2H_5)]^-$, in which the porphyrin is also somewhat more buckled. As usual, the individual pyrrole rings of the porphyrin are almost planar. The dihedral angles between the adjacent mean planes range from 0.4 (2) to 13.0 (2)°, the mean value being 6.6°. Agreements between chemically equivalent bond distances and bond angles within the porphyrin ring and the four pivalamide pickets are satisfactory. The mean values of the chemically equivalent bond distances and bond angles

(24) Bounab, B.; Ricard, L.; Fischer, J.; Weiss, R. Unpublished results. See also ref 25.
(25) Nasri, H.; Fischer, J.; Weiss, R.; Bill, E.; Trautwein, A. X. *J. Am. Chem. Soc.* **1987**, *109*, 2549.
(26) Tang, S. C.; Koch, S.; Papaefthymiou, G. G.; Foner, S.; Frankel, R. B.; Ibers, J. A.; Holm, R. H. *J. Am. Chem. Soc.* **1976**, *98*, 2414.

Table II. Positional Parameters and Their Estimated Standard Deviations[a]

atom	x	y	z	B, Å²	atom	x	y	z	B, Å²
Fe	0.76467 (5)	0.06969 (5)	0.46325 (6)	4.44 (3)	N57	0.5770 (3)	0.0174 (3)	0.2004 (3)	6.5 (2)
S	0.6949 (1)	0.0488 (1)	0.5333 (1)	7.27 (6)	C58	0.5337 (4)	−0.0233 (4)	0.1851 (5)	7.5 (3)
CE1	0.6425 (4)	−0.0034 (5)	0.4760 (6)	9.7 (3)	O59	0.5158 (3)	−0.0465 (4)	0.1215 (4)	13.0 (2)
CE2	0.5930 (4)	−0.0184 (5)	0.5176 (7)	11.4 (4)	C60	0.5078 (4)	−0.0408 (4)	0.2512 (5)	7.9 (3)
C1	0.8455 (3)	−0.0415 (3)	0.5127 (4)	4.4 (2)	C61	0.5050 (4)	0.0129 (5)	0.3055 (5)	9.6 (3)
C2	0.8931 (3)	−0.0636 (3)	0.5744 (4)	5.7 (2)	C62	0.5464 (5)	−0.0930 (5)	0.2960 (6)	10.5 (3)
C3	0.9108 (3)	−0.0153 (3)	0.6215 (4)	5.9 (2)	C63	0.4442 (5)	−0.0656 (6)	0.2185 (7)	12.3 (4)
C4	0.8753 (3)	0.0362 (3)	0.5910 (4)	4.5 (2)	C64	0.8366 (3)	−0.1435 (3)	0.4462 (4)	4.8 (2)
C5	0.8796 (3)	0.0950 (3)	0.6227 (4)	4.5 (2)	C65	0.8748 (4)	−0.1570 (3)	0.3998 (4)	6.5 (2)
C6	0.8451 (3)	0.1452 (3)	0.5944 (4)	4.6 (2)	C66	0.8940 (4)	−0.2173 (4)	0.3933 (5)	7.2 (5)
C7	0.8493 (4)	0.2056 (3)	0.6290 (4)	5.9 (2)	C67	0.8752 (4)	−0.2631 (4)	0.4331 (5)	7.1 (2)
C8	0.8095 (4)	0.2414 (3)	0.5839 (4)	6.1 (2)	C68	0.8375 (4)	−0.2506 (3)	0.4804 (4)	6.4 (2)
C9	0.7805 (3)	0.2045 (3)	0.5197 (4)	4.8 (2)	C69	0.8195 (3)	−0.1914 (3)	0.4878 (4)	5.5 (2)
C10	0.7387 (3)	0.2270 (3)	0.4562 (4)	5.2 (2)	N70	0.7818 (3)	−0.1753 (3)	0.5352 (3)	6.2 (2)
C11	0.7142 (3)	0.1922 (3)	0.3885 (4)	5.1 (2)	C71	0.7665 (4)	−0.2089 (4)	0.5895 (5)	8.3 (3)
C12	0.6752 (4)	0.2173 (4)	0.3202 (4)	7.2 (2)	O72	0.7971 (5)	−0.2569 (5)	0.6185 (6)	7.4 (3)
C13	0.6657 (4)	0.1715 (4)	0.2675 (4)	6.6 (2)	C73	0.7244 (4)	−0.1811 (4)	0.6349 (5)	8.2 (3)
C14	0.6954 (3)	0.1174 (3)	0.3030 (4)	4.8 (2)	C74	0.7411 (7)	−0.1153 (8)	0.6509 (9)	7.7 (5)
C15	0.6936 (3)	0.0602 (3)	0.2685 (4)	4.4 (2)	C75	0.6661 (8)	−0.183 (1)	0.589 (1)	12.1 (7)
C16	0.7196 (3)	0.0068 (3)	0.3039 (4)	4.7 (2)	C76	0.738 (1)	−0.221 (1)	0.712 (1)	14.5 (8)
C17	0.7186 (3)	−0.0512 (3)	0.2667 (4)	5.6 (2)	Na	0.9406 (1)	0.1493 (2)	0.2525 (2)	7.21 (9)
C18	0.7515 (3)	−0.0914 (3)	0.3182 (4)	5.4 (2)	N77	0.9345 (4)	0.2112 (4)	0.3899 (5)	11.1 (3)
C19	0.7744 (3)	−0.0560 (3)	0.3865 (4)	4.6 (2)	C78	0.9701 (8)	0.2668 (7)	0.3964 (9)	23.8 (6)
C20	0.8169 (3)	−0.0788 (3)	0.4503 (4)	4.5 (2)	C79	1.0199 (7)	0.2648 (6)	0.3671 (6)	15.6 (5)
N21	0.8356 (2)	0.0191 (2)	0.5229 (3)	4.0 (1)	O80	1.0180 (4)	0.2341 (4)	0.3013 (5)	18.3 (3)
N22	0.8005 (2)	0.1455 (2)	0.5269 (3)	4.3 (1)	C81	1.0642 (6)	0.2299 (6)	0.2665 (9)	16.0 (5)
N23	0.7249 (2)	0.1320 (2)	0.3779 (3)	4.6 (1)	C82	1.0825 (5)	0.1774 (7)	0.2489 (9)	15.9 (5)
N24	0.7529 (2)	0.0023 (2)	0.3789 (3)	4.1 (1)	O83	1.0432 (3)	0.1306 (3)	0.2319 (4)	9.8 (2)
C25	0.9255 (3)	0.1064 (3)	0.6953 (4)	5.0 (2)	C84	1.0556 (6)	0.0916 (7)	0.1792 (7)	13.6 (5)
C26	0.9820 (4)	0.1187 (4)	0.6923 (4)	6.9 (2)	C85	1.0098 (7)	0.0538 (7)	0.1482 (8)	17.7 (6)
C27	1.0259 (4)	0.1347 (5)	0.7575 (5)	7.9 (3)	N86	0.9498 (4)	0.0766 (4)	0.1286 (4)	9.4 (2)
C28	1.0100 (4)	0.1350 (5)	0.8273 (5)	8.7 (3)	C87	0.9433 (6)	0.1170 (7)	0.0655 (6)	14.6 (5)
C29	0.9541 (4)	0.1228 (4)	0.8325 (5)	8.1 (3)	C88	0.8945 (5)	0.1588 (6)	0.0505 (5)	11.8 (4)
C30	0.9119 (3)	0.1064 (4)	0.7667 (4)	6.0 (2)	O89	0.8952 (3)	0.1947 (4)	0.1172 (4)	12.0 (2)
N31	0.8530 (3)	0.0930 (3)	0.7681 (3)	7.2 (2)	C90	0.8461 (7)	0.228 (1)	0.1158 (8)	23.5 (8)
C32	0.8263 (4)	0.0817 (5)	0.8256 (4)	9.0 (3)	C91	0.8184 (6)	0.2304 (7)	0.1753 (8)	15.0 (5)
O33	0.8557 (4)	0.0807 (6)	0.8915 (4)	19.6 (4)	O92	0.8499 (3)	0.2136 (4)	0.2467 (4)	14.6 (3)
C34	0.7620 (4)	0.0666 (5)	0.8071 (5)	8.4 (3)	C93	0.8370 (6)	0.2417 (8)	0.3102 (7)	17.3 (5)
C35	0.7285 (5)	0.1094 (7)	0.7465 (6)	13.6 (5)	C94	0.8773 (7)	0.2320 (8)	0.3824 (7)	16.8 (5)
C36	0.7409 (5)	0.0753 (6)	0.8793 (6)	12.9 (4)	C95	0.9056 (6)	0.0287 (6)	0.1158 (7)	18.4 (4)
C37	0.7535 (6)	0.0047 (6)	0.7778 (7)	15.6 (4)	C96	0.8901 (6)	0.0081 (6)	0.1860 (7)	18.3 (4)
C38	0.7197 (4)	0.2917 (3)	0.4597 (4)	6.2 (2)	O97	0.8755 (3)	0.0553 (3)	0.2304 (4)	12.6 (2)
C39	0.7543 (4)	0.3398 (4)	0.4428 (5)	8.7 (3)	C98	0.8695 (6)	0.0278 (6)	0.2992 (8)	16.2 (4)
C40	0.7374 (5)	0.4006 (4)	0.4547 (6)	10.5 (3)	C99	0.9182 (6)	0.0275 (5)	0.3625 (7)	13.0 (4)
C41	0.6889 (5)	0.4126 (4)	0.4823 (6)	10.4 (3)	O100	0.9460 (3)	0.0836 (3)	0.3752 (3)	10.4 (2)
C42	0.6553 (4)	0.3666 (4)	0.4979 (6)	9.1 (3)	C101	0.9451 (6)	0.1106 (6)	0.4462 (6)	14.3 (4)
C43	0.6689 (4)	0.3070 (4)	0.4852 (5)	7.1 (2)	C102	0.9509 (9)	0.1687 (8)	0.4509 (6)	20.9 (7)
N44	0.6345 (3)	0.2574 (3)	0.4997 (4)	8.6 (2)	Cl1	−0.0035 (4)	0.2937 (4)	0.7299 (5)	16.4 (3)*
C45	0.5786 (4)	0.2579 (5)	0.5120 (5)	8.4 (3)	C103	−0.0359 (6)	0.3385 (7)	0.6634 (8)	14.9 (4)*
O46	0.5546 (3)	0.3056 (3)	0.5181 (4)	11.9 (2)	C104	−0.0922 (6)	0.3630 (7)	0.6759 (8)	15.0 (5)*
C47	0.5500 (4)	0.1934 (5)	0.5142 (6)	9.7 (3)	C105	−0.143 (1)	0.400 (1)	0.663 (1)	23.3 (8)*
C48	0.5567 (5)	0.1539 (6)	0.4441 (7)	11.8 (4)	C106	−0.1140 (7)	0.4083 (8)	0.5821 (9)	17.3 (5)*
C49	0.4863 (5)	0.2034 (7)	0.513 (1)	17.7 (6)	C107	−0.0651 (6)	0.3946 (7)	0.5457 (8)	15.0 (5)*
C50	0.5816 (6)	0.1579 (6)	0.5866 (6)	12.9 (4)	C108	−0.0195 (7)	0.3550 (7)	0.6017 (9)	16.5 (5)*
C51	0.6687 (3)	0.0583 (3)	0.1828 (4)	5.0 (2)	O72′	0.7661 (7)	−0.2654 (7)	0.5811 (8)	11.5 (4)*
C52	0.7031 (4)	0.0783 (4)	0.1360 (4)	6.3 (2)	C74′	0.692 (1)	−0.123 (1)	0.607 (2)	15.2 (9)*
C53	0.6844 (4)	0.0795 (4)	0.0567 (4)	7.4 (2)	C75′	0.677 (1)	−0.234 (1)	0.646 (2)	14.4 (9)*
C54	0.6296 (5)	0.0597 (4)	0.0258 (4)	8.3 (3)	C76′	0.754 (1)	−0.177 (1)	0.722 (1)	12.6 (7)*
C55	0.5912 (4)	0.0381 (4)	0.0698 (4)	7.3 (2)	Cl2	−0.0680 (9)	0.320 (1)	0.762 (1)	37.3 (9)*
C56	0.6115 (3)	0.0374 (4)	0.1509 (4)	5.8 (2)					

[a] Starred values denote atoms refined isotropically. Anisotropically refined atoms are given in the form of the isotropic equivalent displacement parameter defined as $^4/_3[a^2\beta_{11} + b^2\beta_{22} + c^2\beta_{33} + ac(\cos\beta)\beta_{13}]$.

within these units are given in Table III. The C–S and C–C bond distances and the S–C–C bond angle in the ethanethiolate axial ligand present the expected values (Table III).[27] The average values of the Na–N, Na–O, N–C, C–O, and C–C bond distances are similar to those found in other published structures.[28]

Electronic and Hyperfine Structure. Isomer shifts δ and quadrupole splittings ΔE_Q of the compounds studied here (Table IV) are typical for five-coordinate ferrous high-spin porphyrins; they are especially close to the corresponding values of reduced hemoglobin (Hb)[29] and reduced P450.[30] The isomer shift decreases with increasing temperature according to the second-order Doppler shift.[31] Replacing ligands ($^-SC_2H_5$ by $^-SC_6HF_4$) and cations (Na(⊂18c6) by Na(⊂222)) yields different quadrupole

(27) Hagen, R. S.; Watson, A. D.; Holm, R. H. *J. Am. Chem. Soc.* **1983**, *105*, 3905.
(28) Moras, D.; Weiss, R. *Acta Crystallogr., B* **1973**, *41*, 3879.
(29) Trautwein, A. X.; Alpert, Y.; Maeda, Y.; Marcolin, H. E. *J. Phys.* **1976**, *37*, C6-191.
(30) Sharrock, M.; Debrunner, P. G.; Schulz, C.; Lipscomb, J. D.; Marshall, V.; Gunsalus, I. C. *Biochem. Biophys. Acta* **1976**, *420*, 8.
(31) Gütlich, P.; Link, R.; Trautwein, A. X. In *Mössbauer Spectroscopy in Transition Metal Chemistry*; Springer Verlag: Heidelberg, FRG, 1978; p 67.

Table III. Selected Bond Distances (Å), Bond Angles (deg), and Average Values with their Estimated Standard Deviations

Bond Distances and Angles			
Fe–S	2.324 (2)	Fe–N24	2.076 (4)
Fe–N21	2.066 (4)	⟨Fe–N_p⟩	2.074 (10)
Fe–N22	2.066 (4)	S–CE1	1.803 (7)
Fe–N23	2.088 (4)	CE1–CE2	1.551 (10)
S–Fe–N21	101.4 (1)	S–Fe–N24	105.3 (1)
S–Fe–N22	96.0 (1)	S–CE1–CE2	110.1 (5)
S–Fe–N23	105.8 (1)		
Porphyrin Mean Values[a]			
N–C_α	1.377 (18)	N_{am}–C_{am}	1.344 (23)
C_α–C_β	1.438 (11)	C_{a7}–O	1.234 (46)
C_β–C_β	1.351 (5)	C_{am}–C_{ter}	1.524 (29)
C_α–C_m	1.401 (16)	C_{ter}–C_{ter}	1.516 (49)
C_α–C_{phe}	1.494 (11)	C_{phe}–C_{phe}	1.383 (22)
C_{phe}–N_{am}	1.406 (6)		
C_α–N–C_α	105.8 (8)	C_β–C_α–C_m	124 (1)
N–C_α–C_β	109.9 (9)	C_α–C_m–C_α	125 (1)
C_α–C_β–C_β	107 (1)	C_α–C_m–C_{phe}	117 (1)
N–C_α–C_m	125.4 (8)		
Cryptate [Na(⊂222)]$^+$ Mean Values			
N–C	1.428 (28)	Na···N	2.773 (7), 2.835 (7)
C–C	1.377 (63)	Na···O	2.522 (7)–2.599 (6)
C–O	1.377 (25)		

[a] C_α, C_β, C_m, C_{phe}, N_{am}, C_{am}, and C_{ter} stand for the α, β, methine, phenyl, amido, and *tert*-butyl carbons and nitrogens, respectively.

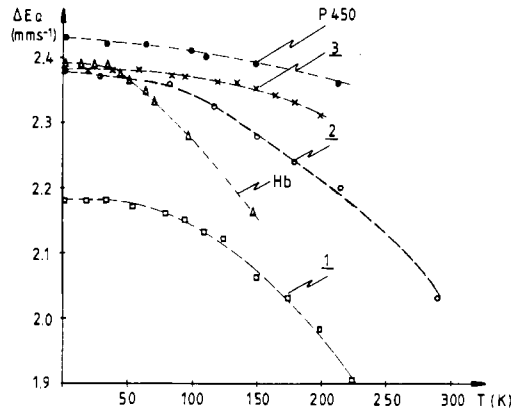

Figure 3. Temperature dependence of quadrupole splittings ΔE_Q of deoxygenated ferrous porphyrin systems: (●) P450, taken from ref 30; (△) Hb, taken from ref 29; (□) **1**; (○) **2**; (×) **3**.

splittings and also a different behavior of its temperature dependence. Compound **3** has an almost temperature-independent ΔE_Q value up to 200 K, and it is in this respect very similar to reduced P450, while **1** and **2** show a slightly temperature-dependent ΔE_Q value that, however, does not vary as much as that of reduced hemoglobin. This behavior indicates that the presence of sulfur as the fifth ligand of the heme iron in reduced P450 and in **1**–**3** gives rise to a stronger tetragonal distortion of the t_{2g} orbitals than the imidazole nitrogen in Hb does.[32] In a deviation from this, the ethanethiolato iron(II) tetraphenylporphyrin complex [Fe(TPP)(SC_2H_5)][Na(⊂222)]·C_6H_5Cl[8] exhibits a pronounced temperature dependence of quadrupole splitting (ΔE_Q = 2.21 mm s^{-1} at 4.2 K, 1.93 mm s^{-1} at 180 K, and 1.76 mm s^{-1} at 215 K) and also of line width (Γ = 0.29 mm s^{-1} at 4.2 K, 0.47 mm s^{-1}at 180 K, and 0.45 mm s^{-1} at 215 K).[33] This situation is comparable to that observed for the dioxygen adduct [Fe($TP_{piv}P$)-(SC_6HF_4)(O_2)][Na(⊂18c6)].[34] These features indicate that the

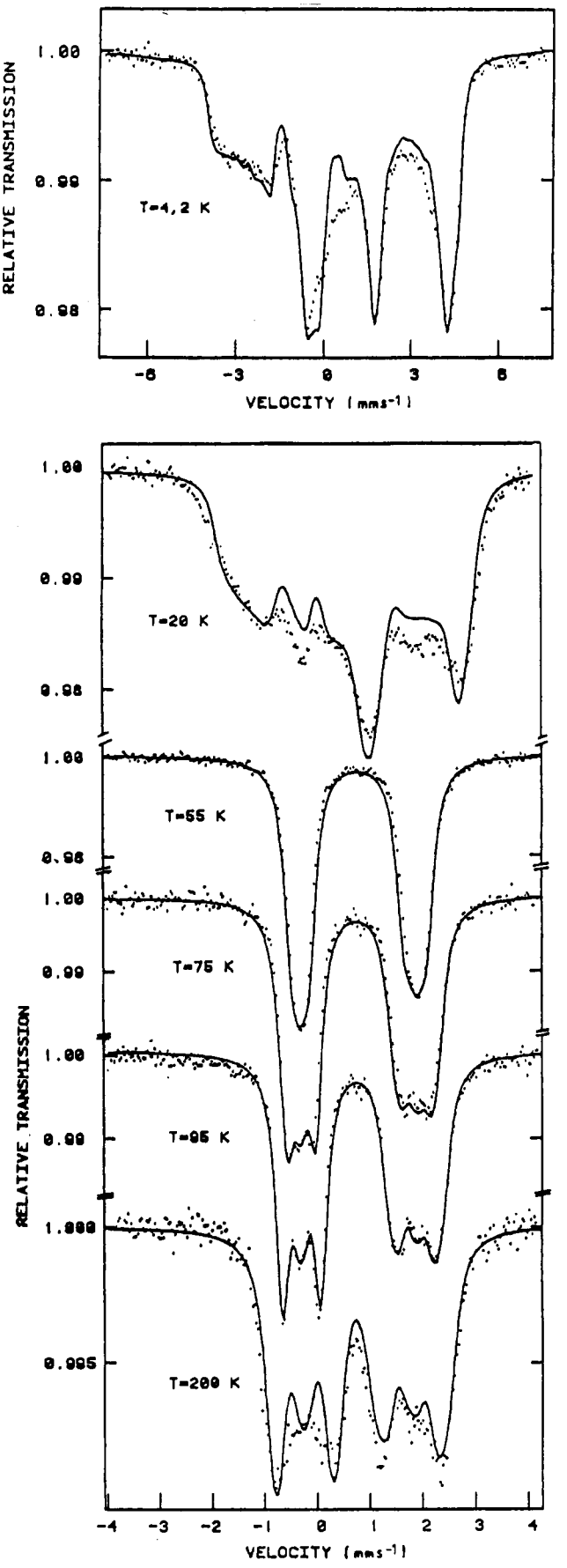

Figure 4. Experimental Mössbauer spectra of **1** under an applied magnetic field (6.4 T, perpendicular to the γ beam) and at various temperatures as indicated. Full lines are simulated spin Hamiltonian spectra from the parameters of Table V in eq 1 and 2.

(32) Montiel-Montoya, R.; Bill, E.; Gonser, U.; Lauer, S.; Trautwein, A. X.; Schappacher, M.; Ricard, L.; Weiss, R. In *The Coordination Chemistry of Metalloenzymes*; NATO-ASI Series C; Bertini, I., Drago, R. S., Luchinat, C., Eds.; D. Reidel: Dordrecht, The Netherlands, 1983; p 363.

(33) Montiel-Montoya, R. Ph.D. Thesis, Universität des Saarlandes, Saarbrücken, FRG, 1983.

Table IV. Isomer Shifts δ (Relative to α-Fe at Room Temperature), Quadrupole Splittings ΔE_Q, and Line Widths Γ at Various Temperatures T for **1–3**[a]

compd	T, K	δ, mm s^{-1}	ΔE_Q, mm s^{-1}	Γ, mm s^{-1}
1	4.2	0.83	2.18	0.30
	20	0.83	2.18	0.29
	35	0.83	2.18	0.29
	55	0.82	2.17	0.29
	78	0.82	2.16	0.29
	95	0.81	2.15	0.28
	110	0.80	2.13	0.29
	125	0.81	2.12	0.29
	150	0.79	2.06	0.30
	175	0.79	2.03	0.30
	200	0.79	1.98	0.31
	225	0.77	1.90	0.31
2	4.2	0.83	2.38	0.32
	30	0.82	2.37	0.32
	77	0.81	2.36	0.32
	115	0.81	2.31	0.38
	150	0.78	2.27	0.36
	180	0.78	2.24	0.34
	215	0.74	2.20	0.34
	290	0.73	2.03	0.46
3	4.2	0.84	2.38	0.28
	20	0.84	2.38	0.30
	40	0.84	2.38	0.30
	60	0.83	2.38	0.30
	85	0.82	2.37	0.27
	95	0.82	2.37	0.28
	120	0.80	2.36	0.25
	135	0.80	2.36	0.25
	150	0.80	2.35	0.28
	165	0.78	2.34	0.28
	180	0.78	2.33	0.26
	200	0.77	2.31	0.26

[a] Standard deviations are ±0.02 mm s^{-1}.

ethanethiolate ligand is bound less rigidly in the tetraphenylporphyrin derivative, as also indicated by the longer Fe–S bond length,[8] compared to the case in the picket-fence porphyrin derivative, where the ethanethiolate ligand lies in the molecular cavity.

We have studied **1** and **3** also under an applied magnetic field (Figures 4 and 5) in order to derive further information from the hyperfine structure of the paramagnetic heme iron, which allows additional comparison with corresponding data derived for reduced P450.[35] The magnetically perturbed experimental Mössbauer spectra we compared with simulated spectra, which were derived by using the usual (electronic) spin Hamiltonian

$$H_{el} = D\left[S_z^2 - \frac{1}{3}S(S+1) + \frac{E}{D}(S_x^2 + S_y^2)\right] + \beta\vec{S}\mathbf{g}\vec{B} \quad (1)$$

with effective spin $S = 2$.

The first term in eq 1 with zero-field splitting parameter D and rhombicity E/D removes the spin degeneracy of the electronic ground state. The second term represents the electronic Zeeman interaction, where **g** denotes the electronic **g** tensor and $\vec{B}$ the applied field. In the present case the ferrous high-spin iron is in the fast-relaxation limit (at least above ca. 15 K); therefore, spin expectation values average thermally over spin states. In the nuclear Hamiltonian H_n we make use of this thermal average, $\langle\vec{S}\rangle_T$, which together with the **A** tensor and the nuclear spin I of ^{57}Fe expresses the magnetic hyperfine interaction $\langle\vec{S}_T\rangle\mathbf{A}\vec{I}$:

$$H_n = \langle\vec{S}\rangle_T\mathbf{A}\vec{I} - g_n\beta_n\vec{B}\vec{I} + H_Q \quad (2)$$

The second term in eq 2 describes the nuclear Zeeman interaction and the third term the electric quadrupole interaction. In our simulation we had to consider the low-symmetry case where the principal axis system (PAS) of the electronic **D** tensor does not coincide with the PAS of the electric field gradient (EFG) tensor; therefore, we had to include three Euler angles (α, β, γ), which rotate the PAS of **D** into the PAS of the EFG tensor. The same procedure was applied by Champion[36] to reduced P450.

From the various spectra recorded for **1** and **3**, respectively, we show some representative examples in Figures 4 and 5 together with simulated spectra using the parameter sets of Table V. Under the present high-field conditions ($B = 6.4$ T) the simulated spectra, obtained in slow- and fast-relaxation limits, respectively, are practically identical for **1** at 4.2 K and for **3** at 1.8 K, because the ground spin state only is populated at these temperatures. Low-field spectra ($B = 0.61$ and 0.93 T) at 4.2 K (not shown here) exhibit typical intermediate-relaxation behavior. Above 15 K the

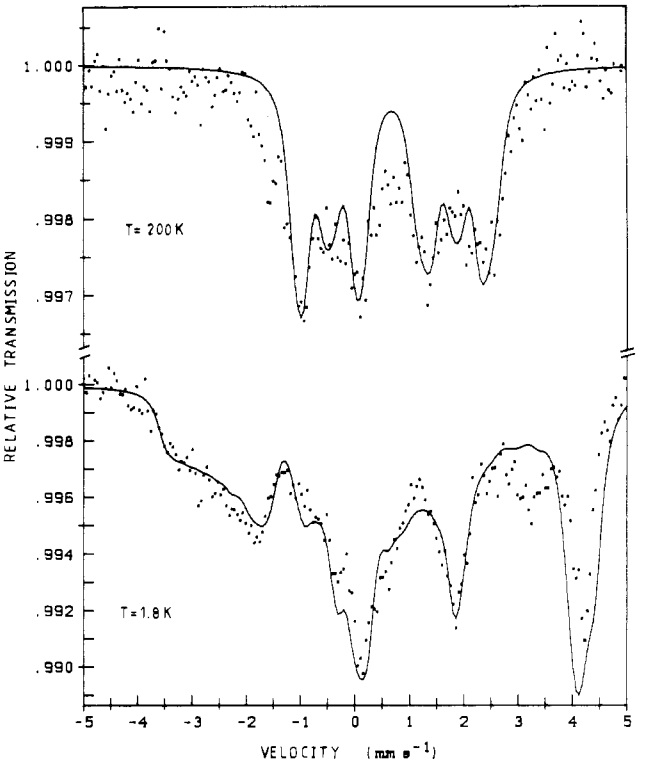

Figure 5. Experimental Mössbauer spectra of **3** under an applied magnetic field (6.4 T perpendicular to the γ beam) and at various temperatures as indicated. Full lines are simulated spin Hamiltonian spectra from the parameters of Table V in eq 1 and 2.

Table V. Parameters Used in the Spin Hamiltonian Simulation (Eq 1 and 2) of Mössbauer Spectra of **1**, **3**, and Reduced P450

	1	**3**	P450[a]
D, cm^{-1}	10.0	8.0	13.9
E/D	0.1	0.18	0.15
δ, mm s^{-1} [b]	0.83	0.84	0.82
ΔE_Q, mm s^{-1} [c]	+2.18	2.38	2.42
Γ, mm s^{-1}	0.30	0.30	0.25
η	0.80	1	0.80
$A_x(T)$	−20.5	−19.0	−18.0
$A_y(T)$	−12.0	−10.0	−12.5
$A_z(T)$	−20.0	−30.0[d]	−15.0
g[d]	2, 2, 2	2, 2, 2	2.24, 2.32, 2
α, β, γ, deg[e]	75, 90, 0	80, 90, 0	60, 70, 0

[a] Taken from ref 5. [b] Relative to α-Fe at room temperature; values correspond to 4.2 K. [c] Values correspond to 4.2 K; the sign corresponds to the main component of the EFG tensor. For simulation at other temperatures the corresponding ΔE_Q values are taken from Table IV. [d] Not sensitive to simulations. [e] Euler angles taking the **D** tensor into the EFG tensor.

(34) Schappacher, M.; Ricard, L.; Fischer, J.; Weiss, R.; Bill, E.; Montiel-Montoya, R. A.; Winkler, H.; Trautwein, A. X. *Eur. J. Biochem.* **1987**, *168*, 419.

(35) Champion, P. M.; Lipscomb, J. D.; Münck, E.; Debrunner, P.; Gunsalus, I. C. *Biochemistry* **1975**, *14*, 4151.

(36) Champion, P. M. Ph.D. Thesis, University of Illinois, Urbana-Champaign, IL, 1975.

spectra are well simulated within the fast-relaxation limit. The fine structure and hyperfine structure parameters derived for **1** and **3** (Table V) agree reasonably well with those found for reduced P450,[35] with no significant preference for **1** or **3**, besides $\Delta E_Q(T)$ for model compound **3** (as mentioned above), which represents the situation in the reduced enzyme closer than **1** does.

Conclusion

The (ethanethiolato)- and (tetrafluorobenzenethiolato)iron(II) picket-fence porphyrin complexes that we have synthesized and characterized are useful models for the reduced ferrous state of cytochrome P450. The Fe–S bond distance of 2.324 (2) Å in the ethanethiolato derivative, which is in complete agreement with the Fe–S bond length found by EXAFS spectroscopy in the reduced ferrous state of P450, shows together with the Mössbauer results obtained for the derivatives studied here that the cysteinate axial ligand remains bound to iron in the ferrous state of cytochrome P450 and is not protonated when reduction of the ferric to the ferrous state of P450 takes place. Oxygenation of some of these complexes led to models for the oxygenated state of cytochrome P450.[13,34,37] The comparison of these structures and Mössbauer properties with the properties of the oxygenated state of P450 led to the conclusion that the cysteinate axial ligand is also bound to iron in the oxy state of the enzyme.[34,37,38]

Acknowledgment. R.W. is a recipient of an Alexander von Humboldt Award and thanks the Alexander von Humboldt Foundation for financial support.

Registry No. **1**, 123411-74-5; **1'**, 123484-33-3; **2**, 123484-31-1; **3**, 123535-87-5; [Fe(TP_{piv})Cl], 86107-94-0.

Supplementary Material Available: Thermal parameters for anisotropic atoms (Table SI), hydrogen atom positions (Table SII), a complete set of bond lengths (Table SIII), a complete set of bond angles (Table SIV), and a full set of experimental X-ray data collection parameters (Table SVI) (17 pages); observed and calculated structure factor amplitudes (×10) for all observed reflections (Table SV) (23 pages). Ordering information is given on any current masthead page.

(37) Schappacher, M.; Ricard, L.; Weiss, R.; Montiel-Montoya, R.; Bill, E.; Gonser, U.; Trautwein, A. X. *J. Am. Chem. Soc.* **1981**, *103*, 7646.
(38) Dawson, J. H.; Kau, L. S.; Penner-Hahn, J. E. Sono, M.; Eble, K. S.; Bruce, G. S.; Hager, L. P.; Hodgson, K. O. *J. Am. Chem. Soc.* **1986**, *108*, 8114.

Contribution from the Institut für Anorganische Chemie, Universität Stuttgart, Pfaffenwaldring 55, D-7000 Stuttgart 80, West Germany

Stabilization of Biochemically Interesting Intermediates by Metal Coordination. 6.[1] Charge Transfer in Complexes of 1,3-Dimethyllumazine with Low-Valent Metals

Christian Bessenbacher,[2] Conny Vogler, and Wolfgang Kaim*

Received March 10, 1989

Chelate complexes between O(4),N(5)-coordinating 1,3-dimethyllumazine and the metal fragments $(Ph_3P)_2Cu^+$, $(bpy)_2Ru^{2+}$ (bpy = 2,2'-bipyridine), and $(OC)_3ClRe$ have metal-to-ligand charge-transfer absorption bands in the visible region. Cyclic voltammetry illustrates the thermodynamic and kinetic stabilization of the reduced state in these complexes.

Flavins, lumazines, and pterins (Chart I) are biochemically important molecules that can function as coenzymes by undergoing 1e- or 2e-transfer reactions coupled with (de)protonation.[3-5] All three heterocycles (Chart I) contain a potentially metal-chelating *α-carbonylpyrazine* coordination site.[6] In the oxidized form, flavins were found to bind only "soft", electron-rich metal centers[7]

Chart I

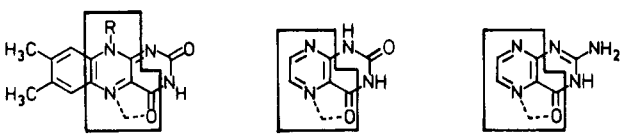

whereas the singly reduced species, the flavosemiquinones, form stable complexes with rather normal metal ions.[8] Complexes of lumazine (2,4(1*H*,3*H*)-pteridinedione) with divalent metal ions were described earlier,[9] and the coordination chemistry of pterins[10] has been discussed recently in the light of the discovery of a "molybdopterin" cofactor,[11] which apparently contains coordinatively linked pterin and molybdenum fragments.

Since the α-carbonylpyrazine moiety represents a strongly π-accepting chelate arrangement,[1,6] the ligands (Chart I) are likely to form compounds with electron-rich metal fragments. Complexes of flavins with Ru(II),[7f-i] Re(I),[6] Ag(I),[7b] and Cu(I)[7c,d] were shown to exhibit structural and spectroscopic effects of

(1) Part 5: Bessenbacher, C.; Ernst, S.; Kohlman, S.; Kaim, W.; Kasack, V.; Roth, E.; Jordanov, J. *J. Chem. Soc., Faraday, Trans. 1*, in press.
(2) Present address: Department of Chemistry, York University, North York, Ontario, Canada M3J 1P3.
(3) (a) Hemmerich, P.; Massey, V.; Wood, H. C. S. *Angew. Chem.* **1965**, *77*, 699; *Angew. Chem., Int. Ed. Engl.* **1965**, *4*, 671. (b) Walsh, C. *Acc. Chem. Res.* **1980**, *13*, 148. (c) Bruice, T. C. *Acc. Chem. Res.* **1980**, *13*, 256. (d) Hemmerich, P.; Massey, V.; Michel, H.; Schug, C. *Struct. Bonding* **1982**, *48*, 93.
(4) Andondonskaja-Renz, B.; Zeitler, H.-J. *Biochem. Clin. Aspects Pteridines* **1984**, *3*, 295. (b) Zeitler, H.-J.; Andondonskaja-Renz, B. *Ibid.* **1984**, *3*, 313.
(5) (a) Scrimgeour, K. G. In *Chemistry and Biology of Pteridines*; Pfleiderer, W., Knappe, W. R., Eds.; de Gruyter: Berlin, 1975; p 731. (b) Dryhurst, G. *Electrochemistry of Biological Molecules*; Academic Press: New York, 1977. (c) Dryhurst, G.; Raghavan, R.; Ege-Serpkenci, D.; Karber, L. G. *Adv. Chem. Ser.* **1982**, *no. 201*, 457. (d) Dix, T. A.; Benkovic, S. J. *Acc. Chem. Res.* **1988**, *21*, 101.
(6) Bessenbacher, C.; Kaim, W. *Z. Anorg. Allg. Chem.*, in press.
(7) (a) Hemmerich, P.; Lauterwein, J. *Inorganic Biochemistry*; In Eichhorn, G. L., Ed.; Elsevier: Amsterdam, 1975. (b) Wade, T. D.; Fritchie, C. J., Jr. *J. Biol. Chem.* **1973**, *248*, 2337. (c) Garland, W. T., Jr.; Fritchie, C. J., Jr. *Ibid.* **1974**, *249*, 2228. (d) Yu, M. W.; Fritchie, C. J., Jr. *Ibid.* **1975**, *250*, 946. (e) Selbin, J.; Sherrill, J.; Bigger, C. H. *Inorg. Chem.* **1974**, *13*, 2544. (f) Clarke, M. J.; Dowling, M. G. *Inorg. Chem.* **1981**, *20*, 3506. (g) Dowling, M. G.; Clarke, M. J. *Inorg. Chim. Acta* **1983**, *78*, 153. (h) Clarke, M. J.; Dowling, M. G.; Garafalo, A. R.; Brennan, T. F. *J. Biol. Chem.* **1980**, *255*, 3472. (i) Clarke, M. J. *Comments Inorg. Chem.* **1984**, *3*, 133.
(8) (a) Müller, G.; Hemmerich, P.; Ehrenberg, A.; Palmer, G.; Massey, V. *Eur. J. Biochem.* **1970**, *14*, 185. (b) Ehrenberg, A.; Müller, F.; Hemmerich, P. *Eur. J. Biochem.* **1967**, *2*, 286. (c) Ehrenberg, A. *Vitam. Horm. (N.Y.)* **1970**, *28*, 489.
(9) Goodgame, M.; Schmidt, M. A. *Inorg. Chim. Acta* **1979**, *36*, 151.
(10) (a) Burgmayer, S. J. N.; Stiefel, E. I. *J. Am. Chem. Soc.* **1986**, *108*, 8310. (b) Kohzuma, T.; Odani, A.; Morita, Y.; Takani, M.; Yamauchi, O. *Inorg. Chem.* **1988**, *27*, 3854.
(11) (a) Rajagopalan, K. V.; Kramer, S.; Gardlik, S. *Polyhedron* **1986**, *5*, 573. (b) Kramer, S. P.; Johnson, J. L.; Ribeiro, A. A.; Millington, D. S.; Rajagopalan, K. V. *J. Biol. Chem.* **1987**, *262*, 16357.

0020-1669/89/1328-4645$01.50/0